level or whether it was due to cascades following the excitation of the $n=4$ and 5 levels as theory suggests [e.g., A. Salop and R. E. Olson, Phys. Rev. A 13, 1312 (1976)].

[2]R. J. Colchin and T. C. Jernigan, J. Nucl. Mater. 63, 83 (1976).

[3]R. H. Dixon and R. C. Elton, Phys. Rev. Lett. 38, 1072 (1977).

[4]R. H. Dixon, J. F. Seely, and R. C. Elton, Phys. Rev. Lett. 40, 122 (1978).

[5]M. J. Seaton, in *Atomic and Molecular Processes*, edited by D. R. Bates (Academic, New York, 1962).

[6]J. Davis, J. Quant, Spectrosc. Radiat. Transfer 14, 549 (1974).

[7]G. A. Martin and W. L. Wiese, Phys. Rev. A 13, 699 (1976).

[8]B. Schiff, C. L. Pekeris, and Y. Accad, Phys. Rev. A 4, 885 (1971).

[9]H. J. Kunze and W. D. Johnson, III, Phys. Rev. A 3, 1384 (1971); W. D. Johnson, III, and H. J. Kunze, Phys. Rev. A 4, 962 (1971).

[10]R. E. Olson, E. J. Shipsey, and J. C. Browne, J. Phys. B 11, 699 (1978).

[11]N. F. Mott and H. S. W. Massey, *The Theory of Atomic Collisions* (Oxford Univ. Press, London, 1965), 3rd ed., Chap. XIX.

[12]Only the inward-flowing impurity ions have been considered in the charge-transfer calculations. If highly stripped ions recycle to the periphery of the plasma, our estimates of the excitation of O^{6+} are low.

Experimental Observation and Numerical Simulations of Laser-Driven Ablation

J. P. Anthes, M. A. Gusinow, and M. Keith Matzen
Sandia Laboratories, Albuquerque, New Mexico 87185
(Received 5 June 1978)

A group of fast ablatively driven ions has been observed by Thomson-parabola and Faraday-cup analyses of an expanding plasma produced by focusing energetic 8-nsec Nd:glass–laser pulses onto thick planar targets. Numerical simulations reveal the formation of an ablation structure with characteristics that agree well with the experimental observations.

With the increasing emphasis on longer laser pulses and ablatively driven targets in laser fusion studies, it is important to gain an understanding of the ablative characteristics of the ion expansion. Long pulses allow sufficient time to establish steady, ablative flow[1,2] from the target surface. In this Letter we report the experimental observation of a characteristic signature of ablation, namely, a group of energetic ablatively driven ions. Calculations have illustrated the formation of this fast-ablation group; the calculated energy of the ablation ions is compared with the experimental measurements.

A Nd:glass–laser system was used for the experiments reported here. The pulses were approximately 8 nsec full width at half maximum (FWHM) and the energy delivered to the target chamber was varied up to 36 J. Pinhole transmission studies similar to those in Ref. 3 gave a focal-spot diameter of 100 μm, defined as containing 90% of the incident energy. The average intensity on target was varied up to approximately 5×10^{13} W/cm^2. (The optical system was effectively $f/5$.) The laser was incident on planar targets (approximately 100 μm thick) at an angle of 17° to the target normal. For the results reported here a Thomson parabola[4] was placed normal to the target surface and a Faraday cup was located 70 cm from the target surface at an angle of 21° from the target normal (38° from the incident laser beam). The background pressure in the target chamber was maintained at less than 3×10^{-6} Torr. Only a small angular dependence was observed when Thomson-parabola traces were obtained simultaneously at both the normal and 21° positions. Although our Thomson parabolas do not measure absolute ion densities,[5] they have been shown to give an accurate measure of the ion energies (± 3%). The ionization stages present in the expanding plasma can be ascertained from the presence of the parabolic traces and qualitative information on the relative densities of the ionization stages can be obtained from the relative brightness of the traces. The results reported here did not vary when a final clean-up dielectric polarizer was removed from the laser. The dielectric polarizer defined p polarization incident on the target. This indicates that resonant absorption is not a significant absorption mechanism in these experiments.

In Figs. 1 and 2(a) Thomson-parabola traces are shown which illustrate the two types of ion expansions observed. The Thomson-parabola device[5] consists of parallel magnetic and electric fields which deflect ions according to their energy (E) and charge state (Z). The electric field

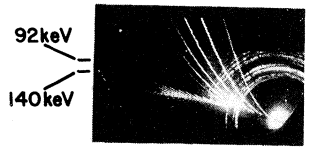

FIG. 1. Thomson-parabola traces produced by focusing 35.6 J on a thick holmium target. The deflection fields were 60 V and 488 G.

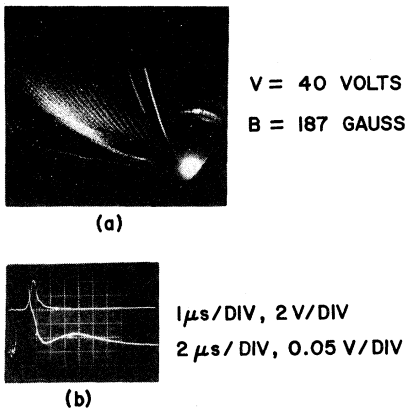

FIG. 2. Thomson-parabola traces (a) and Faraday-cup trace (b) produced by focusing 23.8 J on a thick Ni target. The same trace is displayed twice in (b) with the sweep characteristics as indicated.

deflection (vertical axis) has a Z/E dependence, whereas the magnetic field deflection has a $Z/(EA)^{1/2}$ dependence, where A is the atomic mass. Thus in Fig. 1, the parabolic traces from right to left correspond to species from Ho^{1+} to Ho^{6+}. The individual parabolic traces show the different energies of that particular charge state, with energy increasing towards the origin. A straight line through the origin represents a line of constant velocity. For a target containing only one mass, it also represents a line of constant energy. Thus, the series of ionization stages of Ho which form the traces across the lower part of Fig. 1 represent a group of ions with energy between 92 and 140 keV. The energy values indicated on the left of the figure refer to those lines bounding the energy band of interest here. For these higher ionization stages ($Z > 6$) there are no detectable ions at energies below this energy range. However, the higher-charge-state traces are seen to extend slightly above energies of 140 keV. This Ho trace is typical of traces obtained from heavy elements. A trace typical of low- to intermediate-mass elements is shown in Fig. 2(a). This expanding Ni plasma also exhibits a high density of ions in a relatively narrow energy range. Here, however, these higher ionization stages ($Z > 12$) appear at both higher and lower energies and the lower-charge states ($Z < 12$) do not appear in this energy range. In both instances it is this high density of ions in a relatively narrow energy range that is identified as the signature of laser-driven ablation. Experiments on target materials ranging from Al to U have shown this ablation structure. Experimentally the ablation velocities are observed to depend primarily on incident laser energy with little dependence on target material. In Fig. 2(b) a representative Faraday-cup trace is shown; this trace was obtained on the same shot as Fig. 2(a). Here the fast ablation ions appear as an intense energetic-ion peak at about 1.8 μs (upper trace). The lower-energy lower-ionization-stage plasma results in the less-intense peak at about 9 μs (lower trace).

To model these laser-target interactions we have used a one-dimensional (1-D), two-temperature Lagrangian hydrodynamics and heat-flow code.[6] The target was assumed to be a solid sphere and the majority of the Lagrangian zones are placed in a thin outer shell which is ablated. The laser energy was absorbed in a deposition profile determined by classical inverse bremsstrahlung with the fractional absorption set to its experimentally determined value[7] [(85–93)% for the energies used here]. The Sesame equation of state tables[8] were used. This model is then a 1-D spherical approximation to finite-spot-size flat-target behavior. Spherical symmetry is a more realistic representation of the plasma expansion than is planar symmetry and is required in order to establish the ablative structure and characteristics.[2]

A velocity profile of the Lagrangian grid points representing a Ni target is shown in Fig. 3 for a time near the peak of an 8-nsec 24-J Gaussian pulse which has been focused to a 100-μm-diam spot. The flatness of the profile near 5×10^7 cm/s indicates that a large amount of mass is traveling at this velocity. This uniform velocity results from the acceleration of the Lagrangian grid points through a steady-state density gradient near the target surface[2] and yields a large peak in the density distribution of the expansion velocities of the ions as shown in Fig. 4. This fast-ion ablation peak corresponds to the high density of ions that are observed in the Thomson-parabola traces and the first large peak in the Faraday-

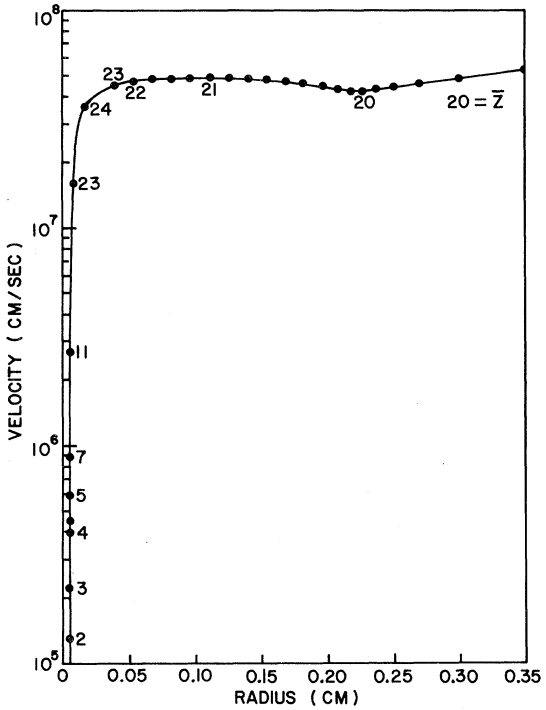

FIG. 3. The velocity profile of the Lagrangian grid points which represent a Ni target at a time (10.6 nsec) near the peak power of 23.8-J 8-nsec–FWHM laser pulse focused to a 100-μm-diam spot. The numbers $\bar{Z}$ represent the equilibrium average ionization stage for that zone as calculated from the Sesame equation-of-state tables.

cup trace. For the Ni shot shown in Fig. 2, the Thomson parabola indicates a high density of ions in the $(4.2-5.8)\times 10^7$-cm/s velocity range, which is in good agreement with the calculated ablation velocity in Fig. 4. The average ionization stages as determined from the Sesame equation of state tables are indicated next to their associated Lagrangian grid points in Fig. 3. The zones that have a velocity near the ablation velocity are seen to have ionization stages ranging from 20 to 24 and the zones at lower velocities have lower average ionization stages. This is also in good qualitative agreement with the traces as observed in Fig. 2. We note, however, that nonequilibrium ionization and recombination processes have not been included in these calculations and they must be included in order to accurately determine charge states present in the expanding plasma.[9]

An illustration of the comparison between theory and experiment is made by dividing the Thomson parabola [Fig. 2(a)], velocity profile (Fig. 3), and ion–expansion-velocity distribution (Fig. 4) into three regions, as indicated schematically in

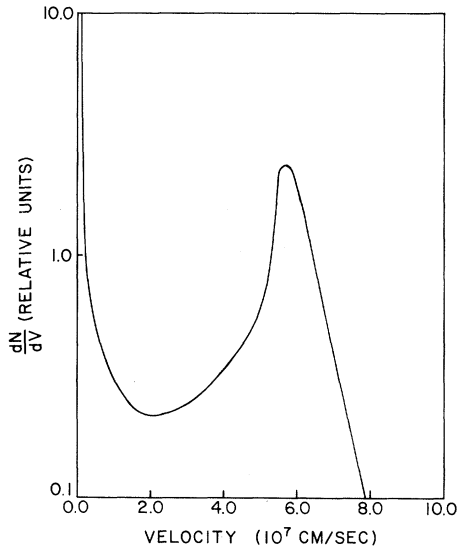

FIG. 4. The density distribution of the ion expansion velocities predicted for the same laser-target parameters as in Fig. 3.

Fig. 5. The central region in each figure represents the ablatively driven ions. The high-energy ions indicated in Fig. 5 (cross-hatched area)

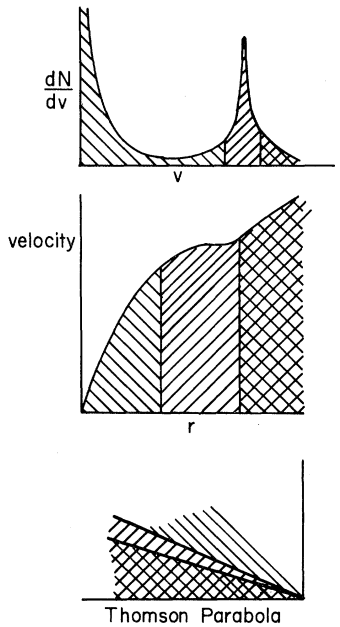

FIG. 5. Schematic representation of the signature of ablation as seen in a density distribution of the ion-expansion velocities, the velocity profile of the plasma expansion, and a Thomson-parabola diagnostic. The ablation region (///) in each representation is between groups of lower (\\\) and higher (cross-hatched) energies.

TABLE I. Comparison of the ion ablation energies from thick Ni targets as a function of incident laser energy.

Laser energy (J)	Ablation energy (keV) Faraday cups	Thomson parabolas	Numerical model
1.4	23	24–30	19
7.0	35	36–78	46
27.7	48	39–80	79

are due to the isothermal plasma expansion which occurs during the initial rise of the laser power. Even-higher-energy ions are observed experimentally which are not predicted by the computation. A possible source of these ions is an early-time electrostatic acceleration of a small group of ions coupled, for example, to the production of fast electrons.

A comparison of the ablation energies as determined from the ion diagnostics and the numerical simulations is shown in Table I for several incident laser energies. The average ablation energy was determined from the time of the fast peak of the Faraday-cup trace and from the position of the ablation peak of the ion-velocity distribution in the numerical simulations. Since it is difficult to select quantitatively the line of maximum ion density in the Thomson parabolas, the range of energies listed in Table I represents the energies of the lines that bound the ablation region. Previous analytic models of ablation[10] have predicted dependences of ion expansion energy on intensity between $I^{1/3}$ and $I^{2/3}$. The exact steady-flow model[1,2] does not predict a single power-law dependence but rather a range of exponents from about 0.5 at low laser intensity to just under 1.0 at high intensity. The numerical simulations (Table I) give a value of the exponent of about 0.55, which is consistent with the steady-flow–model power dependences. Assuming that the focal properties are independent of laser energy, the Faraday-cup measurements show an $I^{0.25}$ dependence. Thus, even though the qualitative features of the formation and velocity structure of the ion expansion are clearly illustrated by the numerical model, the quantitative agreement with experiment could be fortuitous. It is reasonable to expect that two-dimensional effects will be very important with laser pulses 8 nsec in duration. We also emphasize that no attempt was made to improve the quantitative agreement by varying any of the parameters in the code (such as the flux limit and radiation losses) or by including nonequilibrium plasma kinetics.

In summary, we have experimentally observed a group of fast ablatively driven ions. This fast-ion group has been observed in Thomson-parabola and Faraday-cup traces and compares well with the structure and energy predicted by spherical 1-D, hydrodynamic heat-flow calculations.

The authors wish to thank Dr. R. L. Morse for early discussions suggesting that long laser pulses will produce an experimentally observable fast-ion ablation peak and for subsequent informative discussions. We also would like to acknowledge the technical assistance of M. Dillon, F. King, and J. Lavasek. This work was supported by the United States Department of Energy.

[1]S. J. Gitomer, R. L. Morse, and B. S. Newberger, Phys. Fluids 20, 234 (1977).

[2]L. Montierth and R. L. Morse, to be published; M. K. Matzen and R. L. Morse, in the Eighth Annual Conference on Anomalous Absorption of Electromagnetic Waves, Tucson, Arizona, 19–21 April 1978 (unpublished).

[3]J. Anthes, J. Lavasek, and M. Palmer, Sandia Laboratories Report No. SAND 76-0432, September 1976 (unpublished); P. Brannon, J. Anthes, G. Cano, and J. Powell, J. Appl. Phys. 46, 3576 (1975).

[4]J. N. Olsen, G. W. Kuswa, and E. D. Jones, J. Appl. Phys. 44, 2276 (1973).

[5]M. A. Gusinow, G. Lockwood, M. Dillon, and L. Ruggles, Sandia Laboratories Report No. SAND 78-0336, March 1978 (unpublished).

[6]This is a modified version of the code used in R. C. Malone, R. L. McCrory, and R. L. Morse, Phys. Rev. Lett. 34, 721 (1975).

[7]J. P. Anthes, M. A. Palmer, M. A. Gusinow, and M. K. Matzen, to be published.

[8]B. I. Bennett, J. D. Johnson, G. I. Kerley, and G. T. Rood, Los Alamos Scientific Laboratory Report No. La-7130, February 1978 (unpublished).

[9]M. K. Matzen, J. S. Pearlman, and R. L. Morse, Bull. Am. Phys. Soc. 22, 1204 (1977).

[10]E. Cojocaru and P. Mulser, Plasma Phys. 17, 393 (1975); T. R. Jarboe *et al.*, Phys. Fluids 19, 1501 (1976), and references therein.

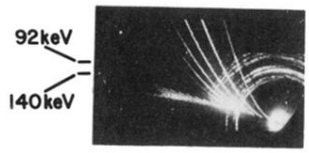

FIG. 1. Thomson-parabola traces produced by focusing 35.6 J on a thick holmium target. The deflection fields were 60 V and 488 G.

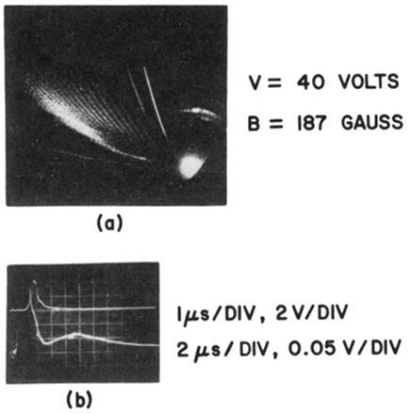

FIG. 2. Thomson-parabola traces (a) and Faraday-cup trace (b) produced by focusing 23.8 J on a thick Ni target. The same trace is displayed twice in (b) with the sweep characteristics as indicated.